

Contribution from the Laboratoire de Chimie Moléculaire, Unité Associée au CNRS, Université de Nice, Parc Valrose, 06034 Nice, France, Rhône-Poulenc, Inc., New Brunswick, New Jersey 08901, Laboratoire de Chimie des Métaux de Transition, UA 419, Université Pierre et Marie Curie, 75252 Paris, France, and Department of Chemistry and Molecular Structure Center, Indiana University, Bloomington, Indiana 47405

## Alcohol Adducts of Alkoxides: Intramolecular Hydrogen Bonding as a General Structural Feature

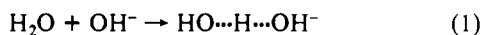
Brian A. Vaartstra,<sup>†</sup> John C. Huffman,<sup>†</sup> Peter S. Gradeff,<sup>‡</sup> Liliane G. Hubert-Pfalzgraf,<sup>§</sup> Jean-Claude Daran,<sup>||</sup> Stephen Parraud,<sup>§</sup> Kenan Yunlu,<sup>†</sup> and Kenneth G. Caulton<sup>\*†</sup>

Received February 12, 1990

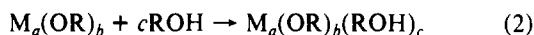
Characterization of  $Zr_2(O^iPr)_8(^iPrOH)_2$  by  $^1H$  and  $^{13}C$  NMR spectroscopy, IR spectroscopy, and single-crystal X-ray diffraction ( $-100$  °C) is reported. The compound crystallizes in the space group  $P\bar{1}$  with  $a = 18.262$  (4) Å,  $b = 19.883$  (5) Å,  $c = 12.067$  (3) Å,  $\alpha = 98.59$  (1)°,  $\beta = 96.26$  (1)°,  $\gamma = 77.49$  (1)°, and  $Z = 4$ . The unit cell contains four half-dimers in the asymmetric unit, all of which differ only in the rotational conformation about Zr-O and O-C bonds. In each dimer, the edge-shared bioctahedron has two  $\mu-O^iPr$  groups. On opposite sides of this  $Zr_2(\mu-OR)_2$  plane, each dimer forms two hydrogen bonds, one each between a coordinated alcohol and a terminal alkoxide. The NMR spectra at 25 °C are so simple as to be structurally uninformative, a result of rapid fluxionality which includes, as one component, proton migration among all  $O^iPr$  units. At  $-80$  °C in toluene, the NMR spectra are now too complex to be accounted for by a single edge-shared bioctahedral structure. The hafnium analogue is isomorphous with the zirconium compound. Although  $Ce_2(O^iPr)_8(^iPrOH)_2$  is not isomorphous, it exhibits an analogous hydrogen-bonded structure in which the O...O distance is as short as it is in the Zr analogue, in spite of a metal-metal separation which is longer by 0.28 Å. It crystallizes in the space group  $P\bar{1}$  with  $a = 11.385$  (4) Å,  $b = 12.144$  (5) Å,  $c = 9.009$  (3) Å,  $\alpha = 109.72$  (1)°,  $\beta = 111.54$  (2)°,  $\gamma = 65.70$  (1)°, and  $Z = 1$ . The generality of hydrogen bonding between M-OR and M-O(H)R groups when they are aligned parallel in a metal cluster is reviewed.

### Introduction

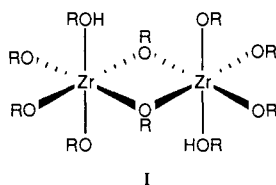
Intramolecular hydrogen bonding involves no loss of the translational entropy found when two particles condense to one in a typical hydrogen bond (eq 1) and thus is a particularly



favorable manifestation of this phenomenon. We wish to point out here that one particularly likely situation for the occurrence of such intramolecular hydrogen bonding is among metal alkoxide compounds, particularly because many metal alkoxide compounds are coordinatively unsaturated and are thus good candidates for coordinating molecular alcohol during their syntheses (eq 2). The



determination that the adduct of empirical formula  $Zr(O^iPr)_4(^iPrOH)$  was a dimer in benzene led Bradley et al.<sup>1</sup> to suggest an edge-shared octahedral structure (I), but without mention of



hydrogen bonding. We report here a single-crystal X-ray diffraction determination of the structure of this and related cerium and hafnium compounds and a general discussion of the occurrence and importance of hydrogen bonding between alcohol and alkoxide ligands.

### Experimental Section

All procedures involved in the preparation and structural characterization of  $M_2(O^iPr)_8(HO^iPr)_2$  were carried out under an atmosphere of dry dinitrogen or argon or in vacuo. All solvents were appropriately dried and distilled prior to use and stored under dinitrogen. The compound  $[Zr(NMe_2)_4]_2$  was prepared according to a modification<sup>2</sup> of the literature procedure.<sup>3</sup> CAN (ceric ammonium nitrate, Rhône-Poulenc) was dried for 72 h in a vacuum oven at 125 Torr and 110 °C.

Table I. Crystal Data for  $Zr_2(O^iPr)_8(^iPrOH)_2$

chem formula	$Zr_2C_{30}H_{72}O_{10}$	fw	775.33
$a$ , Å	18.262 (4)	space group	$P\bar{1}$
$b$ , Å	19.883 (5)	$T$ , °C	$-100$
$c$ , Å	12.067 (3)	$\lambda$ , Å	0.71069
$\alpha$ , deg	98.59 (1)	$\rho_{\text{calc}}$ , g cm <sup>-3</sup>	1.221
$\beta$ , deg	96.26 (1)	$\mu(\text{Mo K}\alpha)$ , cm <sup>-1</sup>	5.26
$\gamma$ , deg	77.49 (1)	$R$	0.0616
$V$ , Å <sup>3</sup>	4216.15	$R_w$	0.0665
$Z$	4		

Infrared spectra were recorded on a Perkin-Elmer 283 spectrometer as solids in Nujol mulls or KBr pellets or as solutions in benzene- $d_6$ . NMR spectra ( $^1H$ ,  $^{13}C\{^1H\}$ ) were recorded on Bruker AM-500, WH-90, and AC-200 and JEOL FX 90Q spectrometers, and chemical shifts were referenced to the protio impurity of the solvent. Cerium was determined as  $CeO_2$  by calcination at 1000 °C.

**Synthesis of  $Zr_2(O^iPr)_8(^iPrOH)_2$ .** Approximately 3 g of  $[Zr(NMe_2)_4]_2$  was dissolved in 20 mL of pentane, and the solution was cooled to 0 °C. To this solution was added 10 mL of 2-propanol, which immediately resulted in rapid gas evolution. After the solution was allowed to stir under dinitrogen for 30 min, it was refluxed for 1 h under slow  $N_2$  purge. The solvent was removed in vacuo, during which time a white microcrystalline solid precipitated. The solid was dried in vacuo for several hours, giving quantitative yields of  $Zr_2(O^iPr)_8(HO^iPr)_2$  as determined by NMR spectroscopy. Single crystals of  $Zr_2(O^iPr)_8(HO^iPr)_2$  suitable for X-ray diffraction studies were obtained by slow diffusion of 2-propanol layered onto a saturated solution of the complex in pentane at  $-20$  °C.

**X-ray Diffraction Study of  $Zr_2(O^iPr)_8(^iPrOH)_2$ .** A suitable crystal was transferred to the goniostat by using standard inert-atmosphere handling techniques and cooled to  $-155$  °C for characterization and data collection. After several samples were mounted and examined, it was discovered that a phase transition was slowly (30 min) occurring. A new sample was then mounted and cooled to  $-100$  °C, and no phase problems occurred.

A systematic search of a limited hemisphere of reciprocal space located a set of diffraction maxima with no symmetry or systematic ab-

\* To whom correspondence should be addressed at Indiana University.

<sup>†</sup> Indiana University.

<sup>‡</sup> Rhône-Poulenc, Inc.

<sup>§</sup> Université de Nice.

<sup>||</sup> Université Pierre et Marie Curie.

- Bradley, D. C.; Mehrotra, R. C.; Swanwick, J. D.; Wardlaw, W. J. *Chem. Soc.* **1953**, 2025. Bradley has reported molecular weight data indicating trimeric and tetrameric aggregation of alcohol-free  $[Zr(O^iPr)_4]_m$  at both the boiling and freezing points of benzene. See: Bradley, D. C.; Holloway, C. E. *J. Chem. Soc.* **1968**, 1316. We emphasize that " $Zr(O^iPr)_4(^iPrOH)$ " and alcohol-free  $[Zr(O^iPr)_4]_m$  are different materials, with different degrees of aggregation, and that the present paper refers only to the former material.
- Chisholm, M. H.; Hammond, C. E.; Huffman, J. C. *Polyhedron* **1988**, *7*, 2515.
- Bradley, D. C.; Thomas, I. M. *J. Chem. Soc.* **1960**, 3857.

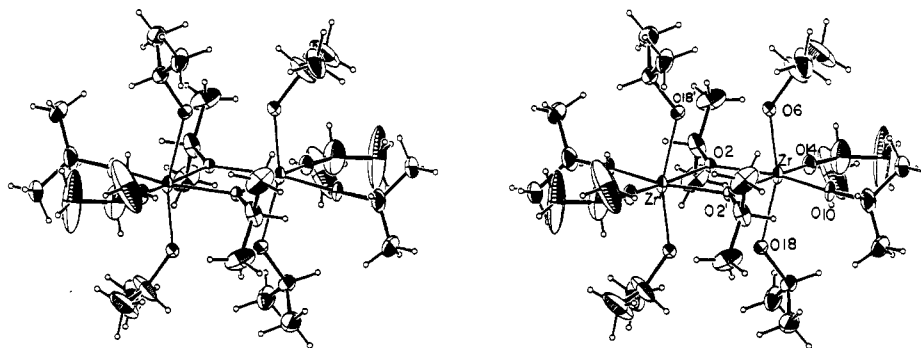


Figure 1. Stereo ORTEP drawing of  $Zr_2(OiPr)_8(iPrOH)_2$ , showing selected atom labeling. Molecule A is portrayed, and primed atoms are related to those not primed by a crystallographic center of symmetry. Thermal ellipsoids are drawn at 50% probability.

Table II. Selected Bond Distances (Å) and Angles (deg) for  $Zr_2(OiPr)_8(iPrOH)_2$

	molecule			
	A	B	C	D
Zr(1)–O(2)	2.166 (4)	2.159 (5)	2.162 (4)	2.159 (4)
Zr(1)–O(2)′	2.180 (4)	2.171 (5)	2.174 (5)	2.191 (4)
Zr(1)–O(6)	2.246 (5)	2.241 (5)	2.287 (5)	2.310 (6)
Zr(1)–O(10)	1.933 (5)	1.937 (5)	1.944 (5)	1.953 (5)
Zr(1)–O(14)	1.939 (5)	1.949 (5)	1.948 (5)	1.944 (5)
Zr(1)–O(18)	2.080 (5)	2.097 (5)	2.049 (5)	2.039 (5)
O(2)–Zr(1)–O(2)′	72.63 (18)	73.02 (19)	72.68 (19)	72.89 (18)
O(2)–Zr(1)–O(6)	77.98 (18)	80.09 (18)	79.10 (19)	78.18 (23)
O(2)′–Zr(1)–O(6)	80.27 (18)	80.05 (18)	77.16 (18)	77.02 (24)
O(2)–Zr(1)–O(10)	166.12 (19)	94.42 (21)	93.11 (20)	164.91 (20)
O(2)′–Zr(1)–O(10)	93.89 (20)	166.72 (21)	162.64 (20)	95.09 (20)
O(2)–Zr(1)–O(14)	95.51 (20)	167.19 (22)	167.18 (21)	93.28 (20)
O(2)′–Zr(1)–O(14)	165.66 (21)	94.86 (22)	95.71 (20)	164.27 (19)
O(2)–Zr(1)–O(18)	86.04 (19)	85.27 (19)	85.39 (20)	87.39 (18)
O(2)′–Zr(1)–O(18)	84.41 (19)	85.09 (19)	88.38 (20)	87.56 (19)
O(6)–Zr(1)–O(10)	93.95 (22)	93.77 (22)	90.64 (22)	91.82 (23)
O(6)–Zr(1)–O(14)	92.32 (22)	93.97 (22)	93.23 (22)	91.65 (25)
O(6)–Zr(1)–O(18)	160.53 (19)	161.61 (19)	161.32 (19)	161.34 (22)
O(10)–Zr(1)–O(14)	97.34 (22)	97.30 (25)	97.27 (22)	97.22 (23)
O(10)–Zr(1)–O(18)	98.21 (23)	98.42 (23)	100.62 (22)	101.47 (21)
O(14)–Zr(1)–O(18)	101.09 (23)	98.06 (22)	99.99 (23)	99.51 (23)
Zr(1)–O(2)–Zr(1)′	107.37 (18)	106.98 (19)	107.32 (19)	107.11 (18)
Zr(1)–O(2)–C(3)	123.2 (5)	126.4 (5)	123.0 (4)	122.2 (4)
Zr(1)′–O(2)–C(3)	129.0 (4)	126.6 (5)	129.6 (4)	130.7 (4)
Zr(1)–O(6)–C(7)	132.1 (5)	130.3 (5)	130.0 (5)	130.6 (5)
Zr(1)–O(10)–C(11)	176.5 (6)	173.8 (7)	168.3 (6)	177.6 (6)
Zr(1)–O(14)–C(15)	167.3 (7)	167.0 (9)	172.7 (6)	170.0 (8)
Zr(1)–O(18)–C(19)	138.8 (7)	131.6 (5)	130.3 (6)	127.8 (5)

sences, corresponding to a triclinic cell. As data were being collected<sup>4</sup> ( $6^\circ \leq 2\theta \leq 45^\circ$ ; see Table I), it became apparent that a pseudo-C-centering was present, and there was some question as to whether or not the proper cell had been chosen.

Data were collected in the usual manner by using a continuous  $\theta$ - $2\theta$  scan with fixed backgrounds. Data were reduced to a unique set of intensities and associated  $\sigma$ 's in the usual manner. All attempts to solve the structure using direct methods and Patterson techniques failed. The structure was finally solved by rejecting the weak data and solving the structure in the nonstandard space group  $C\bar{1}$ . In this space group, two metal atoms were located, each adjacent to a center of inversion. Using this model, it was possible to locate most, but not all, of the remaining atoms by subsequent Fourier techniques. The refinement failed to fall below  $R = 0.21$ .

Using the two Zr locations from the  $C\bar{1}$  cell and two additional Zr atoms at  $1/2, 1/2, 0$  from the located atoms, Fourier techniques were used to solve the structure in  $P\bar{1}$ . All atoms were located, and refinement using blocked diagonal techniques proceeded smoothly. There are four different molecules in the asymmetric unit, each located at a center of inversion. The thermal parameters of one of the half-molecules was fixed in each cycle. By changing which molecule is fixed in successive cycles, we presume no correlation problems are hidden in the blocked diagonal refinement. There is significant thermal motion in the isopropyl groups, and few hydrogens were located. In the final cycles, all nonhydrogen atoms were refined anisotropically, with fixed hydrogen atom contributions.

Table III. Crystallographic Data for  $Ce_2(OiPr)_8(iPrOH)_2$

chem formula	$C_{30}H_{72}O_{10}Ce_2$	fw	873.13
<i>a</i> , Å	11.385 (4)	space group	$P\bar{1}$
<i>b</i> , Å	12.144 (5)	<i>T</i> , °C	–155
<i>c</i> , Å	9.009 (3)	$\lambda$ , Å	0.71069
$\alpha$ , deg	109.72 (1)	$\rho_{\text{calcd}}$ , g cm <sup>–3</sup>	1.408
$\beta$ , deg	111.54 (2)	$\mu(\text{MoK}\alpha)$ , cm <sup>–1</sup>	22.59
$\gamma$ , deg	65.70 (1)	<i>R</i>	0.048
<i>V</i> , Å <sup>3</sup>	1029.97	<i>R</i> <sub>w</sub>	0.052
<i>Z</i>	1		

The results of the structural study are shown in Table II and Figure 1. Further crystallographic details are available as supplementary material.

$[\text{Hf}(\text{O}i\text{Pr})_4(i\text{PrOH})_2]_m$  was synthesized according to the procedure of Bradley et al.<sup>5</sup> IR (Nujol, cm<sup>–1</sup>): 3160 br ( $\nu(\text{OH})$ ), 1342 m, 1182 s, 1185 s, 1163 s, 1129 s, 1024 m, 1015 m, 979 m, 949 m, 824 w, 721 m, 580 w, 542 m, 430 sh ( $\nu(\text{Hf}–\text{OR})$ ), 104. <sup>1</sup>H NMR (CDCl<sub>3</sub>, 25 °C):  $\delta$  6.15 (2), 4.51 (m, 10, <sup>3</sup>J<sub>H–H</sub> = 6 Hz), 1.23 (d, 60, <sup>3</sup>J<sub>H–H</sub> = 6 Hz). <sup>13</sup>C[<sup>1</sup>H] NMR (CDCl<sub>3</sub>, 25 °C):  $\delta$  69.1, 27.3. Crystals suitable for X-ray diffraction were obtained by slow recrystallization from 2-propanol. Cell constants (25 °C): *a* = 18.32 (1) Å, *b* = 19.92 (1) Å, *c* = 12.11 (1) Å,  $\alpha = 97.64 (5)^\circ$ ,  $\beta = 96.72 (5)^\circ$ ,  $\gamma = 78.30 (5)^\circ$ , *V* = 4270 Å<sup>3</sup>.

**Synthesis of  $Ce_2(OiPr)_8(iPrOH)_2$ .** This is an improvement of an earlier method.<sup>6</sup> The earlier report erroneously concluded that DME is coordinated in this product. Sodium isopropoxide was prepared by reacting 25.2 g of Na (1.094 mol) in 220 mL of <sup>i</sup>PrOH and 140 mL of DME at 50 °C. After all of the Na had reacted, 100 mL of DME was added at room temperature. The dark red solution of 100 g of CAN (0.1824 mol) in 140 mL of DME and 120 mL of <sup>i</sup>PrOH was then dropped into the clear solution of the sodium isopropoxide, forming immediately NH<sub>3</sub> gas and a white precipitate. The mixture was stirred overnight and filtered. The precipitate was washed with 100 mL of <sup>i</sup>PrOH and 100 mL of DME to yield 92.5 g of NaNO<sub>3</sub> (theory for 6 NaNO<sub>3</sub>: 93.0 g). The combined filtrates were concentrated until yellow crystals appeared. After 2 days at –30 °C, the dark red supernatant was transferred to another flask by using a syringe and the remaining yellow precipitate was dried at oil-pump vacuum to give 65 g (82%) of a crystalline light yellow material.

Crystals suitable for X-ray structure determination were grown as follows:  $Ce_2(OiPr)_8(iPrOH)_2$  (6.5 g) was dissolved in 30 mL of DME and 20 mL of <sup>i</sup>PrOH and the solution was filtered. The clear, light yellow solution was kept for 2 days at –10 °C, to yield 2 g of light yellow, transparent crystals, mp 100–102 °C.<sup>7</sup> Anal. Calcd for  $Ce_2O_{10}H_{72}C_{30}$ : Ce, 32.13. Found: Ce, 32.52. <sup>1</sup>H NMR (tol-*d*<sub>8</sub>, 27 °C):  $\delta$  1.41 (d, 60, <sup>3</sup>J<sub>H–H</sub> = 6.1 Hz), 4.91 (septet, 10), 6.41 (s, 2). <sup>13</sup>C[<sup>1</sup>H] NMR (tol-*d*<sub>8</sub>, 27 °C):  $\delta$  27.55, 73.92. IR (Nujol, cm<sup>–1</sup>): 1329 m, 1329 w, 1280 w, 1157 sh, 1125 vs, 982 vs, 955 s, 833 m, 822 m, 695 w, 565 m, 520 m, 515 sh, 406 w ( $\nu(\text{Ce}–\text{OR})$ ).

**X-ray Diffraction Study of  $Ce_2(OiPr)_8(iPrOH)_2$ .** A suitable crystal was located and transferred to the goniostat by using standard inert-atmosphere handling techniques and cooled to –155 °C for characterization and data collection. It was necessary to cleave a larger crystal to obtain a sample small enough to minimize absorption. The crystals were

(4) For a general description of diffractometer and crystallographic procedures, see: Huffman, J. C.; Lewis, L. N.; Caulton, K. G. *Inorg. Chem.* **1980**, *19*, 2755.

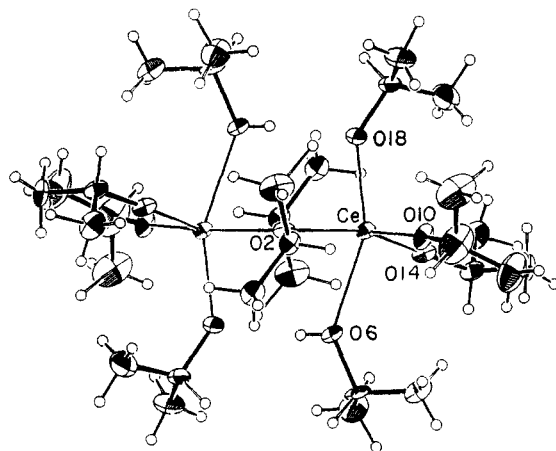
(5) Bradley, D. C.; Mehrotra, R. C.; Wardlaw, W. J. *Chem. Soc.* **1953**, 1634.

(6) Gräff, P. S.; Schreiber, F. G.; Mauermann, H. J. *Less-Common Met.* **1986**, *1*, 26, 335.

(7) Compare: Bradley, D. C.; Chatterjee, A. K.; Wardlaw, W. J. *Chem. Soc.* **1956**, 2260, 3469.

**Table IV.** Selected Bond Distances (Å) and Angles (deg) for  $\text{Ce}_2(\text{O}^i\text{Pr})_8(\text{PrOH})_2$ 

Ce(1)–O(2)	2.325 (6)	Ce(1)–O(10)	2.083 (6)
Ce(1)–O(2)′	2.338 (6)	Ce(1)–O(14)	2.093 (6)
Ce(1)–O(6)	2.523 (6)	Ce(1)–O(18)	2.188 (6)
O(2)–Ce(1)–O(2)′	72.09 (21)	O(6)–Ce(1)–O(18)	155.20 (22)
O(2)–Ce(1)–O(6)	71.95 (20)	O(10)–Ce(1)–O(14)	97.81 (23)
O(2)′–Ce(1)–O(6)	78.19 (21)	O(10)–Ce(1)–O(18)	98.81 (23)
O(2)–Ce(1)–O(10)	93.79 (22)	O(14)–Ce(1)–O(18)	106.52 (22)
O(2)′–Ce(1)–O(10)	165.52 (22)	Ce(1)–O(2)–Ce(1)′	107.91 (21)
O(2)–Ce(1)–O(14)	160.98 (21)	Ce(1)–O(2)–C(30)	120.0 (5)
O(2)′–Ce(1)–O(14)	95.04 (21)	Ce(1)′–O(2)–C(3)	130.3 (5)
O(2)–Ce(1)–O(18)	86.42 (21)	Ce(1)–O(6)–C(7)	134.9 (5)
O(2)–Ce(1)–O(18)	83.81 (20)	Ce(1)–O(10)–C(11)	172.1 (8)
O(6)–Ce(1)–O(10)	94.68 (24)	Ce(1)–O(14)–C(15)	166.7 (5)
O(6)–Ce(1)–O(14)	92.04 (22)	Ce(1)–O(18)–C(19)	140.4 (5)

**Figure 2.** ORTEP drawing of  $\text{Ce}_2(\text{O}^i\text{Pr})_8(\text{PrOH})_2$ , showing bending of O(10) and O(14) toward O(6). The molecule is centrosymmetric. Open circles are hydrogen, and unlabeled atoms are carbon. Thermal ellipsoids are drawn at 50% probability.

thermochromic, being slightly yellow at room temperature and transparent at  $-155^\circ\text{C}$ .

A systematic search of a limited hemisphere of reciprocal space located a set of diffraction maxima with no symmetry or systematic absences indicating one of the triclinic space groups. Subsequent solution and refinement of the structure confirmed the centrosymmetric choice,  $P\bar{1}$ .

Data were collected<sup>4</sup> ( $6^\circ < 2\theta < 45^\circ$ ) in the usual manner, using a continuous  $\theta$ - $2\theta$  scan with fixed backgrounds, and were reduced to a unique set of intensities and associated  $\sigma$ 's in the usual manner. Table III shows parameters of the unit cell and data set.

The structure was solved by a combination of direct-methods (MULTAN78) and Fourier techniques. All hydrogen atoms were clearly visible in a difference Fourier synthesis phased on the non-hydrogen parameters. All hydrogen atoms were refined isotropically and non-hydrogen atoms anisotropically in the final cycles. The molecule contains a crystallographic center of inversion. A final difference Fourier was featureless, with three peaks of intensity, 1.3–2.1  $e/\text{\AA}^3$ , located at the Ce position, and all other peaks less than 0.8  $e/\text{\AA}^3$ . An absorption correction based on the measured size of the crystal did not improve the final residuals or difference Fourier and was abandoned.

The results of the structural study are shown in Table IV and Figure 2. Carbon–hydrogen distances range from 0.71 (22) to 1.31 (13) Å; the O(6)–H(8) distance is 0.75 (12) Å.

## Results

**Zirconium(IV) Isopropoxide.** (a) **Synthesis and Spectral Data.** Alcoholysis of  $[\text{Zr}(\text{NMe}_2)_4]_2$  using 2-propanol proves to be a convenient and high-yield route to  $\text{Zr}_2(\text{O}^i\text{Pr})_8(\text{HO}^i\text{Pr})_2$ . Refluxing the reaction mixture under  $\text{N}_2$  purge is required in order to expel all of the dimethylamine, which appears to be easily incorporated into the product, even upon prolonged evacuation of the solid. If this is not done, the product shows ( $^1\text{H}$  NMR) small amounts of coordinated amine or amide.

In the solid state,  $\text{Zr}_2(\text{O}^i\text{Pr})_8(\text{HO}^i\text{Pr})_2$  displays a broad O–H stretch in the infrared spectrum at  $3180\text{ cm}^{-1}$ . In benzene- $d_6$  solution, the O–H stretch is likewise broad and occurs at  $3130\text{ cm}^{-1}$ . These features are typical of hydrogen bonding. NMR

spectra of the compound in toluene- $d_8$  reveal a single average environment for the isopropyl groups at ambient temperature. The  $^{13}\text{C}\{^1\text{H}\}$  NMR spectrum displays singlets at  $\delta$  26.60 and 69.78 integrating 2:1, respectively. Similarly, the  $^1\text{H}$  NMR spectrum displays a doublet ( $^3J_{\text{H-H}} = 5.5\text{ Hz}$ ) at  $\delta$  1.36 and a broad resonance at  $\delta$  4.54 integrating 6:1, respectively. A very broad alcohol proton resonance is observed at  $\delta$  6.3. Such a large downfield shift is consistent with hydrogen bonding. As the sample is cooled in the NMR probe in toluene- $d_8$ , the spectra become more complex and, at  $-80^\circ\text{C}$ , at least 11 different isopropyl group environments are evident, yet without resolution of the methine proton resonances. At this temperature the OH hydrogen is extremely broad at 5.9 ppm.

**(b) Solid-State Structure.** The material of empirical formula  $\text{Zr}(\text{O}^i\text{Pr})_4(\text{PrOH})$  crystallizes from cold pentane/2-propanol in a unit cell that contains a remarkable four crystallographically independent, centrosymmetric dimers,  $\text{Zr}_2(\text{O}^i\text{Pr})_8(\text{PrOH})_2$ . The general structural features of the  $\text{Zr}_2\text{O}_{10}$  portion of the four independent molecules are nearly identical. The four differ primarily in the rotational conformation about those Zr–O and O–C bonds trans to the bridging alkoxides. Thus, distinct conformers coexist in the solid state.

The structure (Figure 1) is generally that proposed by Bradley et al.<sup>1</sup> (I) with one alcohol ligand on each zirconium and on opposite sides of the  $(\text{RO})_2\text{Zr}(\mu\text{-OR})_2\text{Zr}(\text{OR})_2$  plane. In that plane, the Zr–( $\mu\text{-OR}$ ) distances (average 2.170 Å) are considerably longer than the Zr–O (terminal) distances (average 1.943 Å). These terminal alkoxy groups are also nearly linear at oxygen (average angle Zr–O–C:  $171.7^\circ$ ), consistent with strong O→Zr  $\pi$ -donation. The bonding environments at both of the oxygens of the  $\mu\text{-OR}$  groups are planar; the angles around these oxygens sum to 359.7, 359.9, and  $360.0^\circ$  (twice).

Perpendicular to this  $(\text{RO})_2\text{Zr}(\mu\text{-OR})_2\text{Zr}(\text{OR})_2$  plane, the geometry is considerably distorted from that expected for an edge-shared biotetrahedron. Thus, these "axial" OR and ROH ligands bend markedly toward each other, in spite of the long (nonbonding) Zr···Zr' separations, which range from 3.480 to 3.502 Å. This "leaning" of the axial groups decreases the O···O separations to 2.76–2.78 Å. The average Zr'–Zr–O<sup>i</sup>Pr angle is  $85.3^\circ$ , while the average Zr'–Zr–O(H)<sup>i</sup>Pr angle is  $75.9^\circ$ . Thus, the more weakly bonded ligand (alcohol) bends more. Although hydrogen atoms could not be located in final difference maps, we interpret this bending as evidence of formation of a hydrogen bond between alkoxide and alcohol ligands on both sides of the  $\text{Zr}_2(\text{O}^i\text{Pr})_6$  plane.<sup>8</sup> Note that all <sup>i</sup>Pr groups on these axial ligands point away from the center of the molecule, thus confirming that the (unseen) hydroxylic hydrogen lies generally in the region between the two oxygens. The rotational conformation about the Zr–O bond of these ligands does not vary among the four independent molecules.

The Zr–O bond lengths of these "axial" ligands are sufficiently different as to permit clear identification of alkoxide (average Zr–O = 2.066 Å) and alcohol (average Zr–O = 2.271 Å) groups. This is consistent with the hydrogen bond being asymmetric; i.e., the hydrogen is not equidistant between the two oxygens. There is, however, no significant difference in Zr–O–C bond angles involving alcohol (average value  $130.8^\circ$ ) and the axial alkoxide (average value  $132.1^\circ$ ) ligands.

**Hafnium(IV) Isopropoxide.** For the sake of completeness, we have also investigated hafnium(IV) isopropoxide as it is recrystallized from <sup>i</sup>PrOH. The compound has spectral properties very close to those of the zirconium analogue. The unit cell constants at  $25^\circ\text{C}$  show it to be isomorphous with the Zr analogue and thus a dimer also. Since we anticipated no major differences in bond lengths or angles for the Hf compound compared to the Zr compound, we discontinued our X-ray work on Hf.

**Cerium(IV) Isopropoxide.** (a) **Synthesis and Spectral Data.** The synthesis proceeds in high yield from commercially available

(8) Such "leaning" is wholly absent in the structure of  $\text{Nb}_2(\text{OMe})_{10}$ , where hydrogen bonding is, of course, absent: Pinkerton, A. A.; Schwarzenbach, D.; Hubert-Pfalzgraf, L. G.; Riess, J. G. *Inorg. Chem.* **1976**, *15*, 1196.

ceric ammonium nitrate. The filtration is facilitated by the coarse nature of  $\text{NaNO}_3$ . Recrystallization from 1:1  $\text{MeOC}_2\text{H}_4\text{OMe}$  and  ${}^i\text{PrOH}$  gives a product showing no retention of the ether. In solution, the compound is light sensitive over a period of 1 week in sunlight. Both  ${}^1\text{H}$  and  ${}^{13}\text{C}\{^1\text{H}\}$  NMR spectra ( $\text{CDCl}_3$  or toluene- $d_6$ , 27 °C) show only one environment for all  ${}^i\text{Pr}$  groups in the molecule. The question of structure was resolved by X-ray diffraction.

**(b) Solid-State Structure.** The material of empirical formula  $\text{Ce}(\text{O}^i\text{Pr})_4(\text{}^i\text{PrOH})$  crystallizes (Figure 2) as a centrosymmetric dimer with molecular structure identical with that of the zirconium analogue, but the cerium crystals obtained from DME/2-propanol are *not* isomorphous with those of the zirconium compound. The Ce–O–C angles trans to the bridging alkoxides are nearly linear (average angle 169.4°) and these Ce–O bonds (average 2.088 Å) are the shortest in the molecule. The bridging oxygens are coplanar with their attached groups (angles sum to 358.2°). Slightly longer Ce–O distances are involved in the bonding to those alkoxide ligands which participate in intramolecular hydrogen bonding (Ce–O = 2.188 (6) Å). These are, in turn, 0.34 Å shorter than the Ce–O bonds associated with the coordinated alcohol ligand. Although the hydroxylic hydrogen atom (H(8)) was located for the cerium compound, its refinement to a distance of 0.75 (12) Å from O(6) is certainly not very accurate, and comparison of the O(6)···O(18) distances is therefore more meaningful. While the Ce(1)–Ce(1') distance, 3.770 (2) Å, is longer than the corresponding value in the Zr analogue, the O(6)···O(18)' hydrogen-bridged distance (2.748 (14) Å) is shorter than in the Zr analogue. This is accomplished by greater bending of both the alkoxide (Ce(1)'–Ce(1)–O(18) = 83.96 (8)°) and the alcohol (Ce(1)'–Ce(1)–O(6) = 71.44 (6)°) ligands in the cerium compound. As in the Zr compound, it is the (more weakly bonded) alcohol ligand that bends more. A consequence of the great difference of the Ce–O(6) and Ce–O(18) distances is that the Ce–O(10)–O(14) plane bends (see Figure 2) significantly toward the more weakly bound alcohol ligand (O(6)). This same distortion is present, but to a lesser extent, in the zirconium analogue.

**Removal of Coordinated  ${}^i\text{PrOH}$ .** The tendency for retention of coordinated  ${}^i\text{PrOH}$  should not be overestimated for any of the compounds discussed here. We have in all cases chosen  ${}^i\text{PrOH}$  as one of the components of the recrystallization solvent pair. Recrystallization of  $\text{Hf}_2(\text{O}^i\text{Pr})_8(\text{}^i\text{PrOH})_2$  from cyclohexane yields alcohol-free  $[\text{Hf}(\text{O}^i\text{Pr})_4]_m$ .  $\text{Ce}_2(\text{O}^i\text{Pr})_8(\text{}^i\text{PrOH})_2$  loses the coordinated alcohol when subjected to a vacuum of  $10^{-3}$ – $10^{-6}$  Torr at room temperature or by slurring in  $\text{CH}_3\text{CN}$ , which removes the  ${}^i\text{PrOH}$  molecules but does not itself coordinate. The infrared spectrum of  $\text{Ce}_2(\text{O}^i\text{Pr})_8(\text{}^i\text{PrOH})_2$  always shows some O–H stretch of free alcohol, an effect that we attribute to easy alcohol loss on grinding.

### Discussion

The molecules  $\text{M}_2(\text{O}^i\text{Pr})_8(\text{}^i\text{PrOH})_2$ ,  $\text{M} = \text{Zr, Hf, Ce}$ , have strong structural similarities and owe their structures (e.g., the location of the alcohol ligands) in part to the geometry most efficient for hydrogen bonding. Hydrogen bonding is also indicated by the reduction in energy of the O–H stretching vibration and by its broad appearance, which is typical<sup>9,10</sup> for hydrogen bonding. The presence of the proton, a generally very mobile particle, makes  ${}^1\text{H}$  or  ${}^{13}\text{C}$  NMR spectroscopy less useful than desired for characterizing these compounds. The spectra at 25 °C show only one environment due to rapid proton transfer and consequent site exchange. When low-temperature spectra are recorded in order to halt rapid proton migration, the spectra become more complex than anticipated from the solid-state structure. This we attribute to freezing out of rotamers about the M–O and O–C bonds. This hypothesis is supported by our discovery for zirconium that distinct rotamers actually co-exist in the solid state.

The M–O(alkoxide) distances involving cerium are uniformly 0.14 ( $\pm 0.02$ ) Å longer than those to zirconium. Taking this as an estimate of the inherent difference in metal size, it is of interest that the M–O(H)R distance is 0.25 Å longer for  $\text{M} = \text{Ce}$  than for  $\text{M} = \text{Zr}$ . This indicates the weaker binding of 2-propanol to Ce(IV) than Zr(IV) under comparable circumstances, in spite of the supplementary effects of essentially identical hydrogen bonding in both compounds. Thus, there is no indication that tighter binding of alcohol causes a strengthening of the hydrogen bond (using O···O distance as the criterion).

Extensive studies<sup>11–13</sup> of the structure and reactivity of  $\text{W}_2\text{Cl}_4(\mu\text{-OR})_2(\text{OR})_2(\text{ROH})_2$  compounds reveal a pattern of intramolecular hydrogen bonding between syn OR and ROH groups (linked by a W=W bond) very similar to that in  $\text{Zr}_2(\text{O}^i\text{Pr})_8(\text{}^i\text{PrOH})_2$ . The hydrogen linking the oxygens was not located, but their positioning was deduced from the W–O distances of the ROHOR<sup>–</sup> unit. Depending on the nature of R, symmetric or slightly asymmetric (maximum difference 0.08 Å) hydrogen bonding was inferred. A qualitatively similar situation exists in  $\text{Ti}_2(\text{OPh})_8(\text{PhOH})_2$ , but here the Ti–O distances suggest a very asymmetric (and thus weak) hydrogen bond.<sup>14</sup> The terminal phenoxides have very short Ti–O bonds (1.789 (9) and 1.842 (11) Å). The oxygens involved in hydrogen bonding bend (Ti–Ti–O = 86.7 and 75.8°) so as to shorten the O···O separation to 2.671 (13) Å, and the associated Ti–O distances are very different (1.884 (10) and 2.200 (11) Å), indicating an asymmetric hydrogen bond. The Ti···Ti distance is 3.309 Å. As observed in the structures reported here, *both* the “alkoxide” and the “alcohol” ligands involved in the ROTiTiO(H)R hydrogen bond are very bent at oxygen (126.9 (8) and 132.2 (10)°, respectively).

In  $\text{Zr}_2(\text{O}^i\text{Pr})_8(\text{}^i\text{PrOH})_2$ , the hydrogen-bonded O···O separation is 0.1 Å longer than that in  $\text{Ti}_2(\text{OPh})_8(\text{PhOH})_2$ , but the difference in M–O(H)R and M–OR distances is only 0.20 Å (compared to 0.32 Å for Ti). Given the fact that the nonbonded M···M distance is 0.2 Å larger for zirconium, we conclude that the hydrogen bonding is actually stronger in the zirconium isopropoxide than in the titanium phenoxide. This may be due more to the change in R group than to the change in metal. However, the hydrogen bonding is weaker than that in  $\text{W}_2\text{Cl}_4(\mu\text{-OR})_2(\text{OR})_2(\text{ROH})_2$ , where the W=W multiple bond provides the energy to bring the oxygens closer together (2.48–2.53 Å).

### Other Examples of Hydrogen Bonding to Coordinated Alkoxide.

The definitive structural characterization of *unsaturated*  $\text{M}_4(\text{OR})_{12}$  ( $\text{M} = \text{Mo, W}$ ) clusters was frustrated by consistent formation of crystals of poor X-ray diffraction behavior.<sup>15</sup> An alcohol adduct,  $\text{Mo}_4(\text{OR})_{12}(\text{ROH})$  ( $\text{R} = \text{CH}_2\text{-}i\text{-Bu}$ ), crystallized satisfactorily and exhibits a nearly planar ROMoMoO(H)R unit. The two crystallographically independent molecules show O···O separations of 2.55 and 2.60 Å (the associated Mo–Mo distances are 2.66 and 2.68 Å) and Mo–Mo–O angles of 85.0 (2)–90.5 (3)°. The orientation of the R groups in both independent molecules directs the hydroxyl proton (not located in the X-ray structure) toward the second oxygen. The Mo–O distances (1.97 (1) and 2.34 (1) Å) suggest an asymmetric positioning of the proton in the hydrogen bond.

Are there examples of alkoxide hydrogen bonding to other acidic hydrogens? For example, can the phenomenon occur between alkoxide and  $\text{R}_2\text{N-H}$  bonds? In  $\text{Mo}_2(\text{OSiMe}_2)_6(\text{NHMe}_2)_2$ ,<sup>16</sup> there is no evidence for such hydrogen bonding, perhaps because the presence of two  $\pi$ -acceptors (Mo and Si) diminishes the lone-pair availability of oxygen. On the other hand, Leonelli has observed<sup>17</sup>

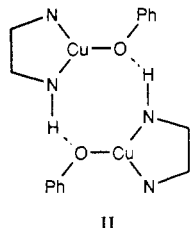
(9) Hamilton, W. C.; Ibers, J. A. *Hydrogen Bonding in Solids*; W. A. Benjamin: New York, 1968.  
 (10) Olovsson, I.; Jönsson, P.-G. In *The Hydrogen Bond*; Schuster, P., Zundel, G., Sandorfer, C., Eds.; North Holland Publishing Co.: New York, 1976; Vol. II.

(11) Harwood, W. S.; DeMarco, D.; Walton, R. A. *Inorg. Chem.* **1984**, *23*, 3077.  
 (12) Cotton, F. A.; DeMarco, D.; Falvello, L. R.; Walton, R. A. *J. Am. Chem. Soc.* **1982**, *104*, 7375.  
 (13) Cotton, F. A.; Falvello, L. R.; Fredrich, M. F.; DeMarco, D.; Walton, R. A. *J. Am. Chem. Soc.* **1983**, *105*, 3088.  
 (14) Svetich, G. W.; Vogt, A. A. *Acta Crystallogr.* **1972**, *B28*, 1760.  
 (15) Chisholm, M. H.; Folting, K.; Hammond, C. E.; Hampden-Smith, M. J.; Moodley, K. G. *J. Am. Chem. Soc.* **1989**, *111*, 5300.  
 (16) Chisholm, M. H.; Cotton, F. A.; Extine, M. W.; Reichert, W. W. *J. Am. Chem. Soc.* **1978**, *100*, 153.  
 (17) Leonelli, J. Ph.D. Thesis, Indiana University, 1982.

that  $[W(O^iPr)_3(NHMe_2)]_2$  exists in the solid state as a nearly eclipsed conformer without any bridging ligands. The N-H bond of each  $NHMe_2$  group points toward an oxygen on the other tungsten, and these N...O distances (2.75 Å) are short because of small W'WN (90°) and W'WO (99°) angles. The other four  $O^iPr$  groups have larger W'WO angles (102–110°).

Tatz<sup>18</sup> has characterized  $[Mo(OCH_2^iBu)_2(NHMe_2)_2]_2$ . In the solid state, this molecule has an eclipsed structure (no bridging alkoxides) which places each N opposite an oxygen, with the hydrogen directed toward that oxygen. The N...O distance (2.7 Å) is consistent with the simultaneous formation of four  $Me_2N-H-OR$  hydrogen bonds.  $[Mo(O^iPr)_2(^iPrOH)_2]_2$  shows similar behavior.<sup>18</sup>

The ligand *N,N'*-di-*tert*-butylethylenediamine, with two secondary amine protons as potential donors, forms a copper(I) phenoxide complex (II) which involves hydrogen bonds.<sup>19</sup> These



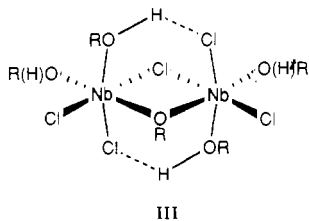
II

hydrogen bonds alone are responsible for this molecule existing as a dimer, since the Cu...Cu separation is nonbonding at 3.17 Å. Mayer<sup>20</sup> has argued that late-transition-metal alkoxides should have particularly electron-rich oxygen centers because the high d-electron count for such metals will minimize the O→M π-donation, which can compete with hydrogen bonding.

Is there analogous hydrogen bonding in monometallic compounds?  $Mo(OSiMe_3)_4(NHMe_2)_2$  shows no evidence for hydrogen bonding between cis  $OSiMe_3$  and  $NHMe_2$  ligands.<sup>21</sup> The same is true for  $Mo(1\text{-adamantoxide})_4(NHMe_2)_2$ .<sup>22</sup>

The face-shared octahedral structure also seems unsuited for intramolecular hydrogen bonding because of a lack of parallel M-L bonds; hydrogen bonding is thus absent in  $Mo_2(OAr)_4(\mu-OAr)_3(NHMe_2)_2$  and  $Mo_2(OAr)_4(\mu-OAr)_2(\mu-NMe_2)(NHMe_2)_2$ .<sup>23</sup>

**Hydrogen Bonding to Other Electron-Pair Donors.** While free chloride ion has been identified as a hydrogen-bond acceptor,<sup>9,10</sup> coordinated chloride also seems to be able to serve the same role. Thus,  $Nb_2Cl_5(O^iPr)(^iPrOH)_4$  (III) has an O...Cl distance of "around 3 Å",<sup>24,25</sup> and an O-H stretching frequency of 3200  $cm^{-1}$ .



III

$[WCl_2[NH^iBu](NH_2^iBu)]_2$  also exhibits intramolecular  $Bu^iNH...Cl$  hydrogen bonding (N...Cl = 3.12 Å) across the  $W=O$  bond, but a detailed analysis is precluded by the occurrence of disorder among the  $NH^iBu$  and  $NH_2^iBu$  groups.<sup>26</sup>

(18) Chisholm, M. H.; Folting, K.; Huffman, J. C.; Tatz, R. *J. Am. Chem. Soc.* **1984**, *106*, 1153.

(19) Haitko, D. In *Biological and Inorganic Copper Chemistry*; Karlin, K. D., Zubieta, J., Eds.; Academic Press: Gunderland, NY, 1986; Vol. II, p 77.

(20) Mayer, J. M. *Comments Inorg. Chem.* **1988**, *8*, 125.

(21) Chisholm, M. H.; Reichert, W. W.; Thornton, P. *J. Am. Chem. Soc.* **1978**, *100*, 2744.

(22) Bochmann, M.; Wilkinson, G.; Young, G. B.; Hursthouse, M. B.; Abdul-Malik, K. M. *J. Chem. Soc., Dalton Trans.* **1980**, 901.

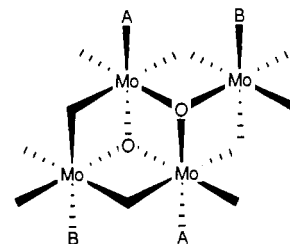
(23) Coffindaffer, T. W.; Niccolai, G. P.; Powell, D.; Rothwell, I. P.; Huffman, J. C. *J. Am. Chem. Soc.* **1985**, *107*, 3572.

(24) Cotton, F. A.; Diebold, M. P.; Roth, W. *J. Inorg. Chem.* **1985**, *24*, 3509.

(25) Cotton, F. A.; Diebold, M. P.; Roth, W. *J. Inorg. Chem.* **1987**, *26*, 3323.

(26) Bradley, D. C.; Errington, R. J.; Hursthouse, M. B.; Short, R. L. *J. Chem. Soc., Dalton Trans.* **1986**, 1305.

Higher valent molybdenum also furnishes a rich array of examples of intramolecular hydrogen bonding.<sup>27–29</sup> The compounds  $Mo_2(N_2Ph)_4Cl_2(\mu-OEt)_2(HOEt)_2$  and  $Mo_2(N_2Ph)_4(\mu-OMe)_2(OMe)_2(H_2NNHPh)_2$  each have long (3.4 Å) Mo-Mo separations, but do display  $Cl...HOEt$  and  $MeO...H_2NNHPh$  hydrogen bonding, the latter involving coordinated phenylhydrazine as the proton source. Tetramolybdenum anions, all of which have the general structure IV, also display the phenomenon. In  $Mo_4O_8-$

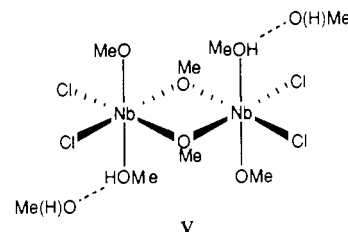


IV

$(\mu-OEt)_2(EtOH)_2Cl_4^{2-}$ ,  $EtOH$  and  $Cl$  hydrogen-bond across A...B. In  $Mo_4O_6Cl_4(O^iPr)_4(^iPrOH)_2$  and  $Mo_4O_8Cl_4(OEt)_2(EtOH)_2^{2-}$ , the same is true, with  $Cl...O$  distances of 3.00 and 3.08 Å, respectively (the  $Mo'-Mo-O$  angle is 82.1°). In  $Mo_4(HB(pz)_3)_2(O)_4(\mu-O)_4(\mu-OMe)_2(MeOH)_2$ , the hydrogen bonding is from  $MeOH$  to  $\mu_2$ -oxide ligands.

Bino has reported<sup>30</sup> the frequent occurrence of  $HOHOH^-$  bridging one metal of each of two  $Mo_3$  triangles. The  $O...O$  distances in such hydrogen bonds range from 2.44 to 2.52 Å. It is thus clear that the hydrogen-bonding moiety in  $M_2(O^iPr)_8(^iPrOH)_2$  is properly written as the *unit*  $ROHOR^-$ , that it is the generalization of the  $HOHOH^-$  unit, and that it can be considered as an intact bidentate ligand, particularly as it approaches a *symmetric* hydrogen bond. In its most general manifestation, then, this is to be thought of as hydrogen bonding between an acid and its conjugate base. Acidity is, of course, enhanced by coordination to a very electropositive metal.

**Exceptions.** In spite of the broad occurrence of  $ROHOR^-$  hydrogen bonding in dinuclear compounds, it can be interrupted by competing effects. Thus,  $Nb_2Cl_4(OMe)_4(MeOH)_2$  adopts a structure<sup>24,31</sup> (V) with a planar  $Nb_2(OMe)_2(MeOH)_2$  substructure



V

seemingly suited to intramolecular hydrogen bonding among axial groups. But, since it has been crystallized with two additional molecules of methanol per formula unit, this lattice methanol is a more potent electron *donor* than the  $Nb-OMe$  oxygen, and so is the favored site for hydrogen bonding. The  $O...O$  distance in this hydrogen bond is long (2.913 Å).

The solid  $Cu_2(en)_2(OPh)_4(PhOH)_2$ <sup>32</sup> might appear to be a candidate for such hydrogen bonds, but instead involves two *five-coordinate* Cu(II) centers with two *lattice* phenols, each of which does hydrogen-bond to a terminal phenoxide ligand (VI). Phenol is also included in the solid lattice upon crystallization of  $Pd(PCy_3)_2(H)(OPh)$ <sup>33</sup> and  $Rh(PMe_3)_3(OPh)$ ,<sup>34</sup> hydrogen bonding

(27) Hsieh, T.-C.; Zubieta, J. *Inorg. Chim. Acta* **1987**, *127*, L31.

(28) Kang, H.; Liu, S.; Shaikh, S. N.; Nicholson, J.; Zubieta, J. *Inorg. Chem.* **1989**, *28*, 920, 2506 (erratum).

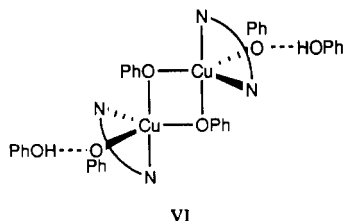
(29) Lincoln, S.; Koch, S. A. *Inorg. Chem.* **1986**, *25*, 1594.

(30) Bino, A.; Gibson, D. *J. Am. Chem. Soc.* **1982**, *104*, 4383.

(31) Cotton, F. A.; Diebold, M. P.; Roth, W. *J. Inorg. Chem.* **1987**, *26*, 3319.

(32) Calderazzo, F.; Marchetti, F.; Dell'Amico, G.; Pellizzi, G.; Colligiani, A. *J. Chem. Soc., Dalton Trans.* **1980**, 1419.

(33) Braga, D.; Sabatino, P.; DiBugno, C.; Leoni, P.; Pasquali, M. *J. Organomet. Chem.* **1987**, *334*, C46.



occurs between coordinated phenoxide and lattice phenol. Co-(Salen)(py)(OMe)-MeOH involves hydrogen bonding from the lattice methanol hydrogen to the coordinated methoxide.<sup>35,36</sup>

**Summary and Generalizations.** This discussion of hydrogen bonding can also be generalized. The phenomenon is most fundamentally one in which an anionic  $M_2(OR)_2^-$  moiety behaves as a bidentate group toward any electrophile. In addition to  $H^+$ , the electrophile could be an alkali-metal cation,  $Tl^+$ ,  $Cu^+$ , or even more highly charged metals:  $CuCl^+$ ,  $HgX^+$ , etc. Compounds of this type (alternatively called intimate ion pairs) have been structurally characterized: (diglyme)NaW<sub>2</sub>H(O<sup>i</sup>Pr)<sub>8</sub>,<sup>37</sup>  $KU_2(O^iBu)_9$ .<sup>38</sup> This generalization also incorporates those cases where a monometallic unit binds cationic electrophiles: (ROH)Li( $\mu$ -OR)<sub>2</sub>Fe(OR)<sub>2</sub> with  $R = CH^iBu_2$ .<sup>39</sup> An extensive network of hydrogen bonding is also observed between the terminal alkoxo groups and the methanol that solvates the cation ( $M = Mg^{2+}$ ,  $Na^+$ ) in compounds such as  $[M(MeOH)_6]_n[Nb_2(OMe)_9]_n$ .<sup>40</sup>

Moving beyond alkoxide chemistry to isoelectronic species, strong amido-ammine hydrogen bonding has been reported between groups positioned on adjacent metals in a Pt(IV)/Pt(IV) dinuclear complex.<sup>41</sup>

The pattern that emerges from the existing body of compounds is that hydrogen bonding will occur when  $M-OR$  and  $M-O(H)R$  vectors lie approximately parallel to one another.<sup>42</sup> Since examples are known with a metal-metal separation as large as 3.8 Å, it is clear that a metal-metal bond is not required.  $M(OR)_3$  compounds (e.g.,  $M = Mo, W, Y, \dots$ ) must aggregate in order to achieve a (preferred) coordination number of 6, and the available degrees of aggregation and associated polyhedra still demand additional neutral ligands. Alcohol is a reactant which is frequently available, as a result of the synthetic procedure, as a solvent when alkoxides are used in material science<sup>43</sup> or in catalysis;<sup>36</sup> it may also be generated by undesirable hydrolysis. Although alkoxides display a limited affinity for binding Lewis bases,<sup>44</sup> alcohol has the advantage over conventional bases of 3-15 kcal/mol from the hydrogen bond; numerous alkoxide-alcohol adducts have been reported and hydrogen bonding must be anticipated. The initial coordination of alcohol may play a critical role for many reactions.<sup>34</sup> More generally, the electron density of the alkoxide oxygen atom might act as an additional "anchor" directed to a four-centered transition state in reactions involving compounds bearing an OH or NH functionality. At the same time, volatile alcohols can be inadvertently removed in subsequent workup, with the result that physical and spectroscopic properties may appear variable as the material is altered from  $[M_a(OR)_b(ROH)_c]_m$  to  $[M_a(OR)_b]_{m'}$ . This is a problem that can plague the discovery and characterization of new binary metal alkoxides.

**Acknowledgment.** We thank the U.S. Department of Energy and the Commissariat à l'Energie Atomique for financial support and Scott Horn for skilled technical assistance.

**Supplementary Material Available:** For  $M_2(O^iPr)_8(PrOH)_2$  ( $M = Zr, Ce$ ), tables of anisotropic thermal parameters, fractional coordinates and isotropic thermal parameters, and full crystallographic details (10 pages); listings of observed and calculated structure factors (27 pages). Ordering information is given on any current masthead page.

- (34) Kegley, S. E.; Schaverien, C. J.; Freudenberger, J. H.; Bergman, R. G.; Nolan, S. P.; Hoff, C. D. *J. Am. Chem. Soc.* **1987**, *109*, 6563.  
 (35) Cesari, M.; Neri, C.; Perago, G.; Perrotti, E.; Zazzetta, A. *Chem. Commun.* **1970**, 276.  
 (36) Bryndza, I. E.; Tam, W. *Chem. Rev.* **1988**, *88*, 1163.  
 (37) Chisholm, M. H.; Huffman, J. C.; Smith, C. A. *J. Am. Chem. Soc.* **1986**, *108*, 222.  
 (38) Cotton, F. A.; Marler, D. O.; Schwotzer, W. *Inorg. Chem.* **1984**, *23*, 4211.  
 (39) Bochmann, M.; Wilkinson, G.; Young, G. B.; Hursthouse, M. B.; Abdul-Malik, K. M. *J. Chem. Soc., Dalton Trans.* **1980**, 1863.  
 (40) Cotton, F. A.; Diebold, M. P.; Roth, W. J. *Inorg. Chem.* **1988**, *27*, 3596.  
 (41) Heck, L.; Ardon, M.; Bino, A.; Zapp, J. *J. Am. Chem. Soc.* **1988**, *110*, 2691.

- (42)<sup>a</sup> For an example where two OMe<sup>-</sup> groups, each of which bridges two metals, can also form a strong hydrogen bond to a single proton, see: Bell, M.; Edwards, A. J.; Hoskins, B. F.; Kachab, E. H.; Robson, R. *J. Am. Chem. Soc.* **1989**, *111*, 3603.  
 (43) Hubert-Pfalzgraf, L. G. *New J. Chem.* **1987**, *11*, 663. Livage, J.; Henry, M.; Sanchez, C. *Prog. Solid State Chem.* **1988**, 259.  
 (44) Hubert-Pfalzgraf, L. G. *Inorg. Chim. Acta* **1975**, *12*, 229. Hubert-Pfalzgraf, L. G.; Riess, G. *J. Chem. Soc., Dalton Trans.* **1974**, 986.

Contribution from 3M Corporate Research Laboratories, St. Paul, Minnesota 55144, and the Department of Chemistry and Molecular Structure Center, Indiana University, Bloomington, Indiana 47405

## Organometallic Chemistry of Fluorocarbon Acids. Structure of $Ti_2(i-PrO)_4(\mu-i-PrO)_2[HC(SO_2CF_3)_2-O,O]_2$ , an Example of an Oxygen-Bonded $HC(SO_2CF_3)_2$ Ligand

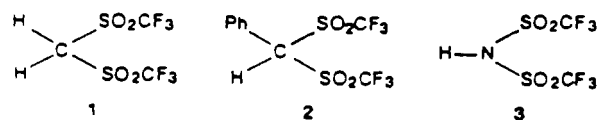
A. R. Siedle\*<sup>†</sup> and J. C. Huffman<sup>†</sup>

Received February 16, 1989

Dimeric  $Ti_2(i-PrO)_4(\mu-i-PrO)_2[HC(SO_2CF_3)_2-O,O]_2$  was obtained from  $(i-PrO)_3TiCl$  and  $Ag[HC(SO_2CF_3)_2]$ . Each titanium atom is bonded to two bridging and two terminal isopropoxy groups. Oxygen atoms, one from each sulfone fragment of the asymmetrically chelating  $HC(SO_2CF_3)_2$  ligand, are also bonded to each titanium with the two Ti-O distances being 2.153 (4) and 2.264 (3) Å. Crystal data (at -155 °C): triclinic,  $P\bar{1}$ ,  $a = 10.384$  (5) Å,  $b = 12.092$  (8) Å,  $c = 10.338$  (6) Å,  $\alpha = 101.99$  (4)°,  $\beta = 119.41$  (3)°,  $\gamma = 99.25$  (3)°,  $Z = 1$ ,  $R(F) = 0.045$ ,  $R_w(F) = 0.0445$ .

### Introduction

We have sought to develop new organometallic chemistry based on the fluorocarbon acids 1-3.<sup>1-10</sup> These materials exhibit a



unique constellation of properties. All are volatile, crystalline solids that are readily soluble in noncoordinating solvents such as toluene

\* 3M Corporate Research Laboratories.

<sup>†</sup> Indiana University.